Chemical-Shift Anisotropy Measurements of Amide and Carbonyl Resonances in a Microcrystalline Protein with Slow Magic-Angle Spinning NMR Spectroscopy

Benjamin J. Wylie, Lindsay J. Sperling, Heather L. Frericks, Gautam J. Shah, W. Trent Franks, and Chad M. Rienstra*

Department of Chemistry, Department of Biochemistry and Center for Biophysics and Computational Biology, University of Illinois at Urbana-Champaign, 600 South Mathews Avenue, Urbana, Illinois 61801

Received January 6, 2007; E-mail: rienstra@scs.uiuc.edu

Chemical shifts are fundamental to interpretation of NMR spectra and provide constraints for macromolecular structure determination, refinement, and validation, as well as details of active-site chemistry in enzymes.[1] Insights into the origins of the chemical shift can be leveraged to improve chemical analysis, including conformation, bonding, and dynamics. To exploit this information fully, it is desirable to measure the full chemical-shift anisotropy (CSA) tensor. Until recently, most efforts to measure backbone amide and carbonyl CSAs have relied upon cross-correlated relaxation and residual anisotropic shifts in solution NMR.[2] Most CSA measurements in solid-state NMR (SSNMR) have customarily been performed in site-specifically labeled peptides, using static powder spectra,[3] single-crystal goniometer experiments,[4] or the slow magic-angle spinning (MAS) method of Herzfeld and Berger.[5] Recoupling techniques utilizing rotor-synchronized radio frequency (rf) pulses[6] tailored for CSA studies of macromolecular solids have recently been extended to 3D experiments suitable for uniformly labeled proteins.[7] These and similar techniques are powerful tools for structural refinement.[8]

Here we demonstrate that the Herzfeld-Berger method can be applied to highly ^{13}C,^{15}N-enriched solid proteins, using 2D heteronuclear correlation in combination with high magnetic fields (750 MHz ^{1}H frequency) and pattern labeling of ^{13}C sites.[9] Slow spinning (3−5 kHz) N−C′ 2D spectra using SPECIFIC CP[10] were acquired using a single sample of GB1,[7] prepared with all ^{15}N sites and most ^{13}C′ labeled as derived from 1,3-^{13}C-glycerol as the sole ^{13}C source in the bacterial growth medium.[9] In such samples, ^{13}C−^{13}C scalar and dipolar couplings are greatly attenuated, enabling the acquisition of 2D ^{15}N−^{13}C sideband manifolds depending primarily upon the CSAs and heteronuclear ^{15}N−^{13}C coupling, parameters which can be readily extracted by comparison to numerical simulations. In each spectrum (Figure 1a), acquired at 3, 4, or 5 kHz MAS, 42 of the 52 expected backbone N−C′ cross-peaks in GB1 in each sideband manifold are resolved; site-specific assignments have been performed previously,[11] as indicated (Figure 1b). Replicate spectra are observed at each sideband order. For example, in the 3 kHz data set, acquired with an ∼18 mg (3 μmol) sample in 18 h of measurement time, 11 ^{13}C′ and 5−6 amide ^{15}N sideband orders are detected. Therefore, for each of the 42 resolved resonances, approximately 50 sideband orders are observed, or a total of ∼2000 independent intensities.

The variations in signal intensities among the manifolds report on site-specific differences in tensor values. For example, in the centerband (0,0) correlation square of the spectrum at 4 kHz MAS, the A48N-D47C′ and Y45N-T44C′ peaks have nearly the same intensity. (We denote the sideband orders i in ^{15}N and j in ^{13}C as (i, j).) In the (−1, +2) region, A48N-D47C′ is 45% stronger than Y45N-T44C′, while in the (−1, −2) region, Y45N-T44C′ is 20% stronger than A48N-D47C′. These intensity variations are an order
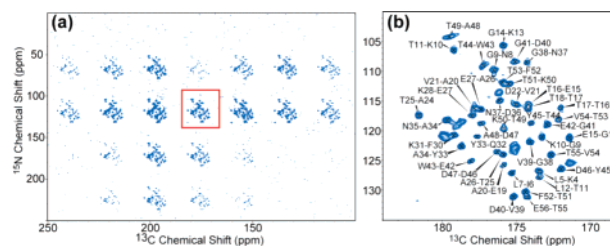

Figure 1. Slow 2D magic-angle spinning (MAS) ^{15}N−^{13}C correlation spectrum of GB1, 750 MHz ^{1}H frequency: (a) full bandwidth 2D plane of N−C′ sideband manifolds at 4 kHz MAS; (b) centerband manifold with resonance assignments indicated.
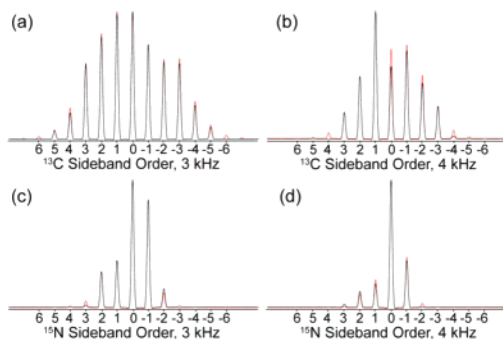

Figure 2. 1D sideband manifolds extracted from the 2D spectra in Figure 1. Spectra are reconstructed by summation of integrated intensities along one dimension. The D40N-V39C′ site is illustrated here. Experimental intensity (black) is simulated (red) by adjusting δ and η, but assuming canonical tensor orientations:[3,4] (a) V39 ^{13}C′, 3 kHz MAS; all ^{15}N sideband orders are summed in this case; (b) V39 ^{13}C′, 4 kHz MAS; (c) D40 amide ^{15}N, 3 kHz, summing over all ^{13}C sideband orders manifold from 3 kHz spectrum; (d) D40 amide ^{15}N, 4 kHz.

of magnitude larger than the random noise in the spectra and, therefore, must be attributable to differences in the tensor parameters. Each set of correlated sidebands at a given site is a function of 10 parameters, which in the Haeberlen convention[12] include the reduced anisotropy δ ($\delta = \delta_{zz} - \delta_{iso}$), the asymmetry parameter η ($\eta = (\delta_{xx} - \delta_{yy})/\delta$), and three Euler angles for each CSA tensor, describing the orientations relative to the ^{15}N−^{13}C dipole vector, which is assumed to be along the peptide bond.

To extract accurate tensor parameters, in the processing we computed 1D representations of the data for each resonance. The total intensity of each sideband order in the x dimension (e.g., ^{13}C) was determined by integrating each peak and summing the integrated peak intensities along the y (e.g., ^{15}N) dimension. This procedure was performed for each sideband order in x and y, resulting in a 1D sideband manifold, as shown in Figure 2. The sideband manifolds were then fit with standard Herzfeld−Berger[5] methods, in our case using a simulation library generated by
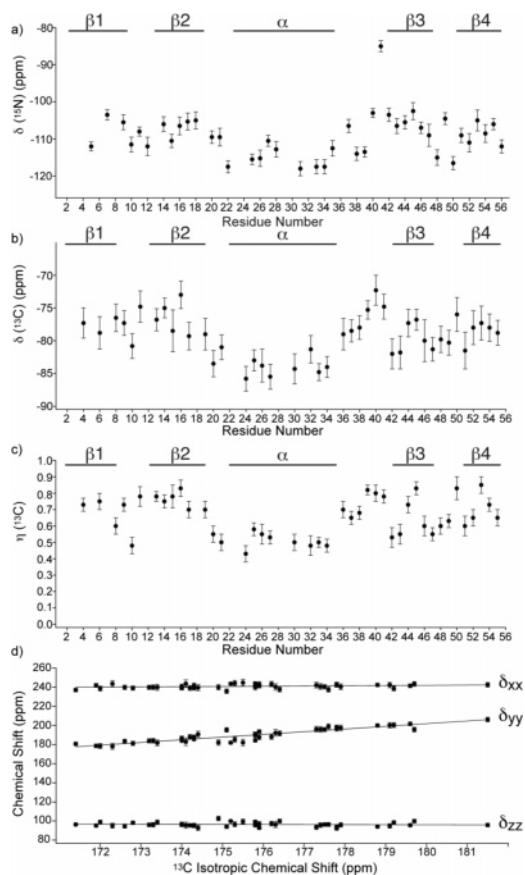
Figure 3. Fitted CSA tensor parameters for GB1; (a) $\delta(^{15}\text{N})$, reduced anisotropy for amide sites; (b) $\delta(^{13}\text{C}')$; (c) $\eta(^{13}\text{C}')$; (d) $^{13}\text{C}'$ principal elements as a function of $^{13}\text{C}'$ isotropic chemical shift.

SPINEVOLUTION.[13] The fitted ^{15}N CSA parameters follow trends in common with our previous measurements performed with ROCSA.[7b] The average value of $\delta(^{15}\text{N})$ throughout the entire protein is -109 ppm, slightly smaller in magnitude for β-sheet residues (-106 ppm) and larger (-115 ppm) in the α-helix (Figure 3a), in excellent agreement with a prior solution NMR study.[2b] The average value of $\eta(^{15}\text{N})$ throughout the protein is 0.2. G41 exhibits a smaller (absolute) value of δ, resulting from dynamics in the α-β3 loop, also evident from $^1\text{H}-^{15}\text{N}$ and $^1\text{H}-^{13}\text{C}$ couplings.[11] In addition, values of δ show greater dependence upon secondary structure compared to many solution studies. Unlike these studies, we did not adjust for molecular motions based upon order parameters. Because such order parameters are based upon scaling of dipolar tensors, it is not clear that such scaling is appropriate for measurements involving (essentially) only one spin.

The measured values for the carbonyl tensors show trends as a function of secondary structure and isotropic chemical shift, with an average $\delta(^{13}\text{C}')$ over the entire protein of -79.3 ppm, -83.5 ppm for helical and -77.7 for β-sheet residues (Figure 3b). The asymmetry parameter η has an even greater dependence upon secondary structure, with an average of 0.53 in α-helical and 0.72 in β-sheet residues and an overall average of 0.65 (Figure 3c). Variations in the isotropic chemical shift are highly correlated with the δ_{yy} tensor element (Figure 3d), in agreement with previous studies.[2b] The additional correlation with $CO\cdots H-N$ hydrogen-bond length[14] suggests that the differences in tensor magnitudes between secondary structural elements are primarily a function of hydrogen bonding, not backbone conformation. In our data, δ_{yy} for $^{13}\text{C}'$ increases linearly with isotropic shift, with a correlation coefficient (R^2) of 0.84 and a slope of 2.82 (Figure 3d). The slope

of the line fitting δ_{xx} versus isotropic shift is an order of magnitude smaller (0.24), and the δ_{zz} value does not vary with isotropic shift (slope of -0.06). In all of these plots, the majority of scatter can be attributed to residues in turns and loops, where greater variations in hydrogen-bond lengths and/or dynamics are likely to be present.

In summary, we have demonstrated that high-quality, slow MAS SSNMR spectra can be acquired in relatively simple experiments employing a diluted-^{13}C labeling scheme in combination with triple resonance experiments at high magnetic fields. In total, three data sets requiring approximately 1 day each of measurement time yielded 42 pairs of ^{15}N and $^{13}\text{C}'$ tensors with straightforward fitting procedures. We envision applications to biological systems by combination with individual or amino acid type-specific labeling. This approach could have particular value for interrogating active sites of enzymes, where hydrogen bonding and hybridization of intermediate states often report directly on mechanistic details. The ability to measure many sites throughout a protein simultaneously in 2D experiments provides important internal controls in this context.

Supporting Information Available: Details of the data acquisition, processing and fitting procedures; tables of measured tensor parameters; full bandwidth spectra at several spinning rates; larger version of Figure 2. This material is available free of charge via the Internet at http://pubs.acs.org.

References

(1) Oldfield, E. *Annu. Rev. Phys. Chem.* **2002**, *53*, 349−378.
(2) (a) Kroenke, C. D.; Rance, M.; Palmer, A. G. *J. Am. Chem. Soc.* **1999**, *121*, 10119−10125. (b) Cornilescu, G.; Bax, A. *J. Am. Chem. Soc.* **2000**, *122*, 10143−10154. (c) Loth, K.; Pelupessy, P.; Bodenhausen, G. *J. Am. Chem. Soc.* **2005**, *127*, 6062−6068. (d) Hall, J. B.; Fushman, D. *J. Am. Chem. Soc.* **2006**, *128*, 7855−7870.
(3) (a) Oas, T. G.; Hartzell, C. J.; McMahon, T. J.; Drobny, G. P.; Dahlquist, F. W. *J. Am. Chem. Soc.* **1987**, *109*, 5956−5962. (b) Oas, T. G.; Hartzell, C. J.; Dahlquist, F. W.; Drobny, G. P. *J. Am. Chem. Soc.* **1987**, *109*, 5962−5966. (c) Hartzell, C. J.; Whitfield, M.; Oas, T. G.; Drobny, G. P. *J. Am. Chem. Soc.* **1987**, *109*, 5966−5969.
(4) (a) Stark, R. E.; Jelinksi, L. W.; Ruben, D. J.; Torchia, D. A.; Griffin, R. G. *J. Magn. Reson.* **1983**, *55*, 266−273. (b) Harbison, G. S.; Jelinksi, L. W.; Stark, R. E.; Torchia, D. A.; Herzfeld, J.; Griffin, R. G. *J. Magn. Reson.* **1984**, *60*, 79−82.
(5) Herzfeld, J.; Berger, A. E. *J. Chem. Phys.* **1980**, *73*, 6021−6030.
(6) (a) Tycko, R.; Dabbagh, G.; Mirau, P. A. *J. Magn. Reson.* **1989**, *85*, 265−274. (b) Liu, S. F.; Mao, J. D.; Schmidt-Rohr, K. *J. Magn. Reson.* **2002**, *155*, 15−28. (c) Chan, J. C. C.; Tycko, R. *J. Chem. Phys.* **2003**, *118*, 8378−8389.
(7) (a) Wylie, B. J.; Franks, W. T.; Graesser, D. T.; Rienstra, C. M. *J. Am. Chem. Soc.* **2005**, *127*, 11946−11947. (b) Wylie, B. J.; Franks, W. T.; Rienstra, C. M. *J. Phys. Chem. B* **2006**, *110*, 10926−10936.
(8) (a) Witter, R.; Sternberg, U.; Ulrich, A. S. *J. Am. Chem. Soc.* **2006**, *128*, 2236−2243. (b) Witter, R.; Sternberg, U.; Hesse, S.; Kondo, T.; Koch, F. T.; Ulrich, A. S. *Macromolecules* **2006**, *39*, 6125−6132.
(9) (a) LeMaster, D. M.; Kushlan, D. M. *J. Am. Chem. Soc.* **1996**, *118*, 9255−9264. (b) Hong, M. *J. Magn. Reson.* **1999**, *139*, 389−401. (c) Castellani, F.; van Rossum, B.; Diehl, A.; Schubert, M.; Rehbein, K.; Oschkinat, H. *Nature* **2002**, *420*, 98−102.
(10) Baldus, M.; Petkova, A. T.; Herzfeld, J. H.; Griffin, R. G. *Mol. Phys.* **1998**, *95*, 1197−1207.
(11) Franks, W. T.; Zhou, D. H.; Wylie, B. J.; Money, B. G.; Graesser, D. T.; Frericks, H. L; Sahota, G.; Rienstra, C. M. *J. Am. Chem. Soc.* **2005**, *127*, 12291−12305.
(12) Haeberlen, U. *High-Resolution NMR in Solids: Selective Averaging.* Academic Press: New York, 1976.
(13) Veshtort, M.; Griffin, R. G. *J. Magn. Reson.* **2006**, *178*, 248−282.
(14) (a) Kameda, T.; Takeda, N.; Kuroki, S.; Kurosu, H.; Ando, S.; Ando, I.; Shoji, A.; Ozaki, T. *J. Mol. Struct.* **1996**, *384*, 17−23. (b) Kameda, T.; Ando, I. *J. Mol. Struct.* **1997**, *412*, 197−203. (c) Wei, Y.; Lee, D.-K.; Ramamoorthy, A. *J. Am. Chem. Soc.* **2001**, *123*, 6118−6126.

JA0701199